IEEE Access
Multidisciplinary | Rapid Review | Open Access Journal

Received September 7, 2018, accepted October 6, 2018, date of publication October 12, 2018, date of current version November 9, 2018.

Digital Object Identifier 10.1109/ACCESS.2018.2875759

Study of Visual Quality Assessment on Pattern Images: Subjective Evaluation and Visual Saliency Effects

TSUNG-JUNG LIU, (Member, IEEE)
Department of Electrical Engineering and Graduate Institute of Communication Engineering, National Chung Hsing University, Taichung 40227, Taiwan
e-mail: tjliu@dragon.nchu.edu.tw

This work was supported by the Ministry of Science and Technology, Taiwan, under Grant MOST 106-2218-E-025-001-MY2.

ABSTRACT This paper presents a comparison study on visual quality scores obtained from single-stimulus and double-stimulus approaches for pattern images, respectively. We also conduct the comparison on general (non-pattern) images, which serve as a control group. The pattern and non-pattern (PNP) images are collected and built by the Perceptual Data Analysis and Processing Laboratory, National Chung Hsing University, and evaluated by a group of people with both single-stimulus and double-stimulus approaches. Then, we examine the difference of mean opinion scores obtained by both the methods with respect to the image types, image contents (scenes), and distortion types. The hypothesis tests are used to determine whether there is a significant difference between both the sets of scores. The test results suggest that the differences exist and are significant for some specific distortion types and image contents. For example, the pattern images with simple colors should be viewed by the double-stimulus method in order to reduce the variance of subjective scores. In the end, we test three well-known full-reference image quality metrics (IQMs) on both the PNP images. In addition, we investigate whether the visual saliency (VS) plays a more important role for pattern images compared with non-pattern images. We discover that the most salient regions are more influential on pattern images than non-pattern images. Also, by introducing the VS information into the IQMs with a newly proposed Otsu's weighted VS mask, the correlation performance between objective quality scores obtained from IQMs and subjective scores from human's visual perception can be boosted further.

INDEX TERMS Absolute category rating-hidden reference (ACR-HR), hypothesis test, pattern images, simultaneous double stimulus for continuous evaluation-discrete category scale (SDSCE-DCS), visual saliency (VS).

I. INTRODUCTION

In recent years, visual quality assessment has drawn considerable attention to many researchers on several topics [1], such as image quality metrics [2]–[6], video quality metrics [7], the construction of image quality databases with specific purpose [8], [9], and new subjective test methods for evaluating image quality [10] and video quality [11]. Among the topics mentioned above, the later two belong to the area of subjective visual quality assessment [12], [13], which plays an irreplaceable role to the development of perceptual quality assessment. Most of these subjective evaluation methods for visual quality assessment have been included into the international standard, such as ITU-R BT.500-13 [14], and ITU-T P.910 [15]. Some of these approaches (e.g., single stimulus continuous quality evaluation (SSCQE) [14], absolute category rating (ACR) [15], and pair comparison (PC) [15]) do not use explicit references. However, the other methods, such as double stimulus continuous quality scale (DSCQS) [14], simultaneous double stimulus for continuous evaluation (SDSCE) [15], and degradation category rating (DCR) [15] use explicit references. Broadly speaking, the SSCQE and ACR belong to single-stimulus approaches. The DSCQS, SDSCE, DCR, and PC are defined as the double-stimulus approaches. Single stimulus is a type of approach where observers rate the quality of only distorted image, while in double stimulus methods, viewers evaluate the quality or the change on quality between two compared images (reference and distortion).

In general, each subjective test methodology has its own advantages and disadvantages. For instance, the

SSCQE approach is claimed to have more representative estimates for quality monitoring applications [16]. The DSCQS method is considered to have less sensitivity to context effects [14] because the images are displayed in pairs with random order. When human subjective opinions are influenced by the order and severity of distortions within the test, the context effects occur. For example, when a strongly distorted image is presented after a series of weakly distorted images, the subjects may rate the image with a lower score than it actually has. Moreover, the SDSCE is a double-stimulus test approach where the subjects view reference and distorted images simultaneously. The two images can be shown side by side on two aligned monitors or on the same monitor depending on the size of the image.

Besides continuous rating scale adopted by SSCQE, DSCQS and SDSCE, ACR and DCR choose the discrete scale, which simplifies the scoring process since the discrete rating scale has much fewer levels than the continuous scale. First, the ACR is fast and can be implemented easily. More importantly, the stimuli presentation of the ACR is similar to that of the common use of the systems. The DCR method can be used when testing the fidelity with respect to the source signal. Moreover, the DCR can also be applied for high quality system evaluation in the context of multimedia communications [15]. The PC approach provides the high discriminating capability, which is particularly useful when test images have similar image quality. However, in order to complete the collection of enough valid results from observers, large numbers of comparisons are necessary. This will discourage its use.

As we know, several specific purpose images have been studied, such as high dynamic range (HDR) images [8], and screen content images [9]. In this work, we would like to investigate whether there exists a difference between the quality scores obtained from subjective test methods without reference and with explicit reference for pattern images. Pattern images belong to a special type of images which have repeated objects or periodic shapes (e.g., concentric circles and squares). Because of this characteristic of self-similarity, it is difficult to distinguish the differences between two similar pattern images. Also, the degradation or distortion happened on repeated objects or periodic shapes in the pattern images may enhance or lessen the personal bad perceptual feeling on image quality. Moreover, pattern images are also widely found in natural scenes and our daily life, such as clouds, trees, building architecture, and clothing. In addition, pattern images were also rarely explored by the researchers. Therefore, we would like to study on pattern images since they are also important to humans.

First, in order to accomplish this task, we collect 30 source images, including 15 pattern and another 15 non-pattern images. Then we generate several types of distorted images with 4 distortion levels based on these 30 reference images. Secondly, we evaluate these images via both ACR with hidden reference (ACR-HR) and SDSCE with discrete category scale (SDSCE-DCS). The results of the subjective evaluation are examined by the steps described in [14], and the scores obtained from outlier viewers are excluded from the calculation of mean opinion score (MOS). We compare the scores from ACR-HR (without explicit reference) and SDSCE-DCS (with explicit reference) methods. In addition, we also discuss how the visual saliency information affects the estimation of visual quality on pattern and non-pattern images for the existing popular objective image quality metrics.

The rest of the paper is organized as follows. First, in Section II, we introduce the source images, and then the two subjective methods (i.e., ACR-HR and SDSCE-DCS) we adopted to evaluate the images. The subjective test procedure is also elaborated in Section II. Afterwards, a thorough comparison between scores obtained from both approaches is conducted and we analyze the differences via statistical tests in Section III. In Section IV, we investigate the impact on the performance of predicting visual quality scores for pattern and non-pattern images by incorporating visual saliency information into image quality metrics. Several visual saliency detection methods are included into the existing image quality metrics for comparison. Finally, the conclusion is drawn in Section V.

II. SUBJECTIVE TESTS

A. PATTERN AND NON-PATTERN IMAGES

In order to investigate if the self-similarity (e.g., repeated objects or periodic shapes) in the image will affect the visual perception of humans toward image quality, we choose the 14 natural images from [17] and one artificial image from [18] as the reference images for this special type of images (called *pattern* images). In addition, to have another type of images for comparison, we select 15 images from the Kodak database [19] as the reference images for this second group of images (called *non-pattern* images). We also can use the following method and steps to classify images into pattern and non-pattern images, respectively. In the first step, we determine whether there exist repeated objects (RO) or periodic shapes (PS) in the image. In the second step, we check if the number of RO or PS is more than 3. The image will be classified as pattern image if both steps are satisfied. Otherwise, the image will be classified as non-pattern image. The flowchart of image classification is demonstrated in Fig. 1.

Next, we generate four commonly seen types of distortion, including Gaussian blur, additive Gaussian white noise, JPEG compression, and contrast change. Thus, the collection of all pattern and non-pattern images constitute the Pattern and Non-Pattern (PNP) image quality database [20], which includes 30 reference images, 4 distortion types for each reference image, and 4 different levels for each distortion type. In another word, the complete database contains 480 distortion images with size 512×384 stored in bitmap (BMP) format. For easy reference, we show 15 reference pattern images (scenes) in Fig. 2 and 15 reference non-pattern images in Fig. 3, respectively. To be able to generate

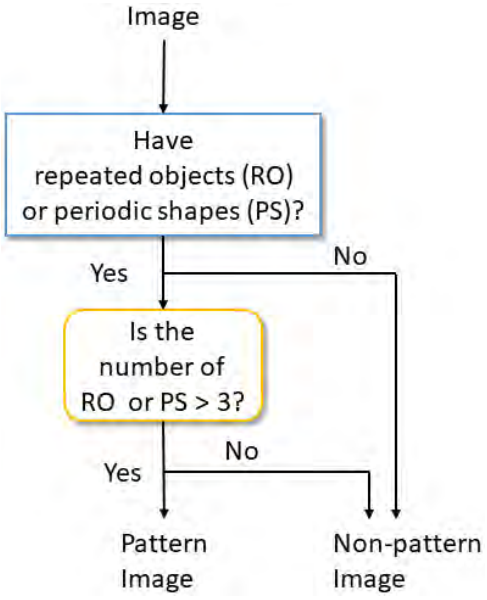

FIGURE 1. Pattern image classification steps.

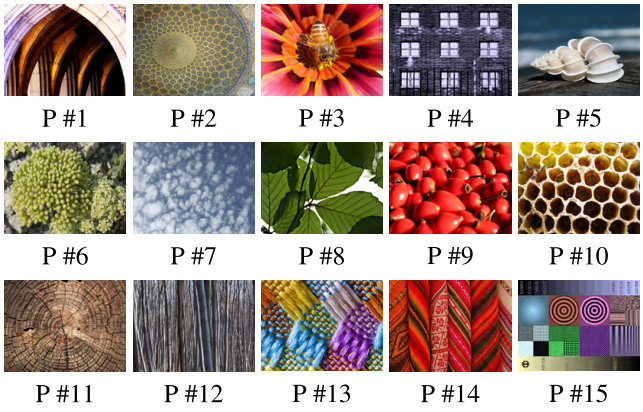

FIGURE 2. Reference images for pattern (P #1 - P #15) images in PNP image quality database.

FIGURE 3. Reference images for non-pattern (NP #1 - NP #15) images in PNP image quality database.

four different visually perceivable levels of distortion for each type of image distortion, we use the following methods and parameters:

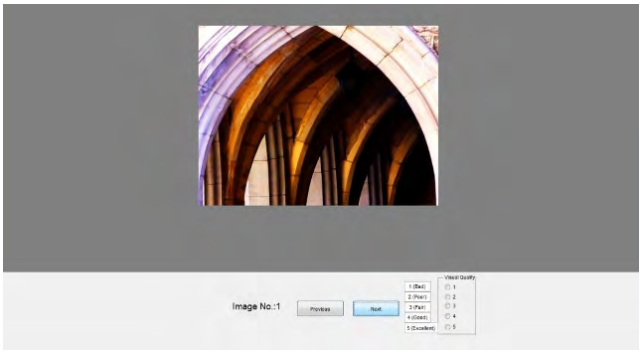

FIGURE 4. The graphical user interface designed for test without reference.

- Gaussian blur:
  Apply a rotationally symmetric Gaussian lowpass filter of 4 different sizes (3×3, 6×6, 9×9, and 12×12) with standard deviation 5 to the original image.
- Additive Gaussian white noise:
  Add Gaussian white noise to the image with zero mean and 4 different variances 0.01, 0.05, 0.1, and 0.5.
- JPEG compression:
  Use Matlab *imwrite* function to generate 4 different lossy compressed images with quality parameters 20, 40, 60, and 80.
- Contrast change:
  Use Matlab *imadjust* function to map 4 different contrast limits ([0.1, 0.9], [0.2, 0.8], [0.3, 0.7], and [0.4, 0.6]) of the original image to the same contrast limit ([0, 1]) of the generated image.

B. SUBJECTIVE TEST WITHOUT REFERENCE

To realize a subjective viewing test without reference for PNP image quality database, the ACR-HR method is chosen since it is easier to implement and able to accommodate more assessments in a single session [21]. Here, the five-level rating scale, labeled as "Bad", "Poor", "Fair", "Good", and "Excellent", is employed in the test. They correspond to numerical score 1 to 5, where the score "5" corresponds to the excellent visual quality, and the score "1" represents the bad visual quality. In the test, the subjects are presented one test image each time, and then asked to give a score (1 to 5) to each viewed image independently. The test procedure must include a reference version of each test image. During the data analysis, a differential quality score will be computed between each test image and its corresponding (hidden) reference. This is known as "hidden reference". The graphical user interface for the subjective evaluation without reference is shown in Fig. 4.

C. SUBJECTIVE TEST WITH REFERENCE

The subjective tests for this part are realized by SDSCE-DCS method. First, as shown in Fig. 5, a test image and the corresponding reference image are simultaneously displayed on the screen. The left image is the source image

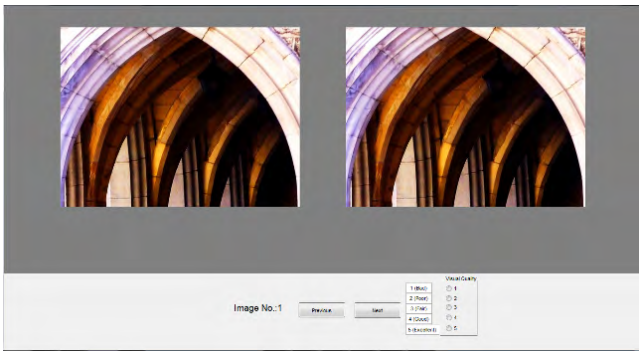

FIGURE 5. The graphical user interface designed for test with reference.

for reference, and the right image is the test image to be evaluated. Next, the test subject is asked to rate the test image based on the reference (undistorted) image with five-level discrete rating scale, which is the same as the one we used in the subjective test without reference. A higher level (e.g., 9 or 11) rating scale can also be used [22]. However, to make the process of scoring simpler for the subjects, the 5-level scale is chosen.

D. TEST EVALUATION PROCEDURE

First, the 480 distorted images are divided into 2 groups (i.e., pattern and non-pattern images), respectively. For each group of images, we conduct the visual quality tests by both ACR-HR and SDSCE-DCS. Therefore, there are 4 test sessions to be conducted in the experiment. This means each subject only has to view 255 (240 distorted images plus 15 reference images) images in one session. The average time cost for each subject in one session is approximately 15 minutes, which will not cause visual fatigue to the viewers [14] and affect the viewing outcomes. Furthermore, we set the color of background to be gray (i.e., pixel value 128) [15] to lessen the visual contrast effect [23].

We also keep the viewing conditions [14], [24] (e.g., peak luminance of the screen, and background room illumination) the same for each viewer. The images are displayed at a Dell 21'' full-color LCD monitor with 1366×768 resolution. And the viewing distance between the center of the screen and the observer is six times the image height (i.e., 6H, where H is the image height).

A training (or demo) session is designed to place before the test session to instruct the viewers how to give a consistent opinion score to the visual quality of each image. All the images in the test session has to be different from those in the training session. Participating viewers (including 17 males and 8 females) in the test are the university students, including undergraduate and graduate students. 21 of the viewers have age ranging from 20 and 29 years old, and the other 4 viewers have age between 30 and 39 years old. In addition, the number of experts and non-experts in the test are 15 and 10, respectively. In the end, 25 sets of scores are recorded for each test image.

E. MEAN SCORE COMPUTATION

After obtaining the scores via both ACR-HR and SDSCE-DCS approaches, we follow the procedure outlined in [14] to obtain the MOS and standard deviation for each test image.

Let S_{ijk} denotes the subjective score given by the observer i to the image j in session $k = \{1, 2, 3, 4\}$. We convert the original raw score S_{ijk} to differential viewer score (DVS) D_{ijk}, which is specified in [15]. Then the DVSs are calculated on per subject and per test image basis. The corresponding hidden-reference (HR) is used to calculate D_{ijk} by the formula below

$$D_{ijk} = S_{ijk} - S_{ij(HR)k} + 5, \tag{1}$$

where $S_{ij(HR)k}$ is the viewer's opinion score for the corresponding hidden-reference (HR). Next, D_{ijk} values will be modified by the following 2-point crushing function to become crushed DVS (CDVS) values C_{ijk}

$$C_{ijk} = \begin{cases} \dfrac{7 + D_{ijk}}{2 + D_{ijk}} & \text{when } D_{ijk} > 5 \\ D_{ijk} & \text{otherwise.} \end{cases} \tag{2}$$

Then the mean score $\bar{C}_{jk}$ and standard deviation σ_{jk} for test image j in the k-th session are

$$\bar{C}_{jk} = \frac{1}{N} \sum_{i=1}^{N} C_{ijk}, \tag{3}$$

$$\sigma_{jk} = \sqrt{\frac{1}{N-1} \sum_{i=1}^{N} \left(C_{ijk} - \bar{C}_{jk}\right)^2}, \tag{4}$$

where N is the number of observers.

To screen out the abnormal observers, the observers screening steps have to be performed as suggested in [14].

1) Determine whether the subjective scores are normally distributed or not by calculating the kurtosis coefficient β_{jk}

$$\beta_{jk} = \frac{m_4}{(m_2)^2} \text{ where } m_x = \frac{\sum_{i=1}^{N} (C_{ijk} - \bar{C}_{jk})^x}{N}, \; x = 2, 4.$$

The scores are considered to be in normal distribution if β_{jk} lies between 2 and 4. Otherwise they are not normally distributed.

2) For each observer i, find L_{ik} and M_{ik} by:
If $2 \le \beta_{jk} \le 4$, then
if $C_{ijk} \ge \bar{C}_{jk} + 2\sigma_{jk}$, then $L_{ik} = L_{ik} + 1$;
if $C_{ijk} \le \bar{C}_{jk} - 2\sigma_{jk}$, then $M_{ik} = M_{ik} + 1$;
else
if $C_{ijk} \ge \bar{C}_{jk} + \sqrt{20}\sigma_{jk}$, then $L_{ik} = L_{ik} + 1$;
if $C_{ijk} \le \bar{C}_{jk} - \sqrt{20}\sigma_{jk}$, then $M_{ik} = M_{ik} + 1$;
end

3) If $\frac{L_{ik}+M_{ik}}{N_{ik}} > 0.05$ and $\left|\frac{L_{ik}-M_{ik}}{L_{ik}+M_{ik}}\right| < 0.3$, then we reject observer i, where N_{ik} is the number of test images seen by the observer i in the k-th session.

TABLE 1. Number of participated and rejected observers in each session.

Test session	1	2	3	4
Image Type	Pattern	Pattern	Non-pattern	Non-pattern
No. of participated observers	25	25	25	25
No. of rejected observers	2	1	0	0
N_k	23	24	25	25

Finally, the values of MOS and the standard deviation (SD) for each test image can be computed by

$$MOS_{jk} = \frac{1}{N_k}\sum_{i=1}^{N_k} C_{ijk}, \tag{5}$$

$$SD_{jk} = \sqrt{\frac{1}{N_k - 1}\sum_{i=1}^{N_k}\left(C_{ijk} - MOS_{jk}\right)^2}, \tag{6}$$

where N_k is the number of remaining observers in the k-th session after observer rejection. Then the MOS and SD values are recorded for each test image. The number of participated and rejected observers in each test session is shown in Table 1. In sessions 1 and 2, the non-pattern images are viewed, while the pattern images are observed in sessions 3 and 4. As we can notice from Table 1, the numbers of rejected observers are 0, 0, 2, and 1 for session 1 to 4, respectively. Thus, more observers are decided as outliers when viewing pattern images.

III. ANALYSIS AND DISCUSSION

In order to observe the differences between the scores obtained by ACR-HR and SDSCE-DCS for both pattern and non-pattern images, we apply the Hypothesis test methods [10], [25] to determine the relationship between two subjective testing methods. The hypothesis tests we used here are paired t-test and Wilcoxon signed-rank test depending on the distribution of subjective scores [26]. In other words, the paired t-test is used when the scores are normally distributed, and the Wilcoxon signed-rank test is adopted otherwise. For both hypothesis tests mentioned above, we reject the null hypothesis if h = 1, where the null hypothesis is

H_0:{No significant difference between 2 MOS groups obtained from ACR-HR and SDSCE-DCS}

with probability $P < \alpha$, where α is the significance level, which is generally chosen as 0.05. In another word, there is a significant difference between two MOS groups if h = 1, while the difference between two MOS groups is not significant if h = 0. We also conduct the difference analysis in terms of three aspects, specifically the image types, image scenes (contents), and image distortion types.

A. IMAGE TYPES

First, we calculate the h value for both pattern and non-pattern images. As indicated in Table 2, the hypothesis testing suggests the significant difference exists between two sets of MOSs obtained by ACR-HR and SDSCE-DCS for pattern images, and also non-pattern images. Hence, observing images with reference or without reference definitely can guide us to give different quality ratings for the image quality. We also can observe that the MOS distributions for both ACR-HR and SDSCE-DCS methods are significantly different in either pattern or non-pattern images from Fig. 6. In addition, by observing Table 3, the sum of variances (SoV) is larger for conducting subjective evaluation by ACR-HR in both pattern and non-pattern images. The difference of SoV between ACR-HR and SDSCE-DCS becomes significant when the evaluation is performed on pattern images. Therefore, we should conduct subjective viewing tests by SDSCE-DCS for both types of images, especially for pattern images.

TABLE 2. The h value (0 or 1) of hypothesis test of MOSs between ACR-HR and SDSCE-DCS for pattern and non-pattern images.

Image Type	Pattern	Non-pattern
h	1	1

TABLE 3. The sum of variances of MOSs between ACR-HR and SDSCE-DCS for both types of images.

Image Type	Pattern		Non-pattern	
Evaluation method	ACR-HR	SDSCE-DCS	ACR-HR	SDSCE-DCS
Sum of variances	168.81	**159.72**	162.24	**161.94**

TABLE 4. The h value (0 or 1) of hypothesis test of MOSs vs. image scenes between ACR-HR and SDSCE-DCS for pattern and non-pattern images.

Image Content #	Pattern	Non-pattern
1	1	0
2	0	0
3	1	0
4	1	0
5	0	0
6	1	0
7	1	1
8	1	1
9	0	0
10	1	0
11	0	0
12	1	0
13	0	0
14	1	0
15	0	1

B. IMAGE SCENES (CONTENTS)

In Table 4, we can notice that the MOSs are significantly different between the ones obtained by ACR-HR and SDSCE-DCS for pattern image with contents #1, #3, #4, #6, #7, #8, #10, #12, and #14. And we can observe these nine pattern images all have repeated patterns and simple colors. Similarly, the h value is also one for non-pattern image with contents #7, #8, and #15, which are a couple, mountain & river, and a house, respectively. It suggests that the difference between the MOSs obtained by ACR-HR and SDSCE-DCS is significant. Thus, the opinion scores of viewers will be very different depending on the existence of the

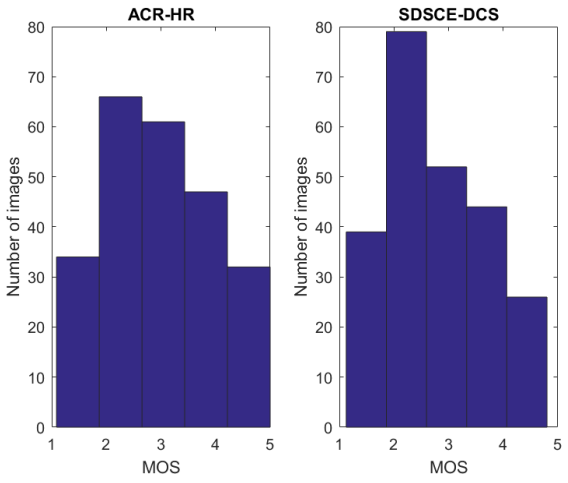

(a)

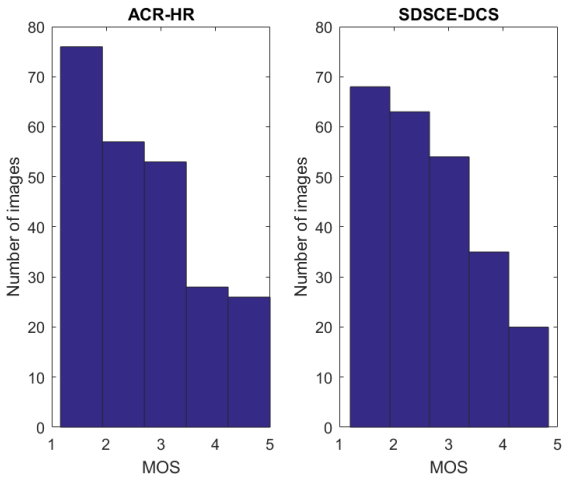

(b)

FIGURE 6. Histograms of MOSs for PNP database. (a) Pattern images. (b) Non-pattern images.

TABLE 5. The sum of variances of MOSs between ACR-HR and SDSCE-DCS for different types of image contents.

Image Content #	Pattern		Non-pattern	
	ACR-HR	SDSCE-DCS	ACR-HR	SDSCE-DCS
1	10.56	**9.14**	10.70	9.44
2	10.68	12.67	9.12	9.18
3	9.83	**9.73**	8.69	11.86
4	11.53	**7.78**	9.59	8.79
5	7.76	8.70	11.68	14.14
6	12.42	**9.12**	10.90	9.99
7	13.94	**11.05**	15.73	**9.40**
8	11.35	**9.64**	14.83	**13.12**
9	13.73	12.54	12.52	9.95
10	**11.51**	14.95	10.27	9.07
11	10.20	14.41	8.48	9.43
12	10.32	**8.16**	10.39	12.48
13	10.87	9.84	8.88	11.11
14	15.26	**12.80**	9.49	13.47
15	8.86	9.20	10.97	**10.51**

reference, especially for image contents with dull colors. Table 5 also suggests there is smaller SoV if we evaluate these images (non-pattern images #7, #8, #15) by SDSCE-DCS.

TABLE 6. The h value (0 or 1) of hypothesis test of MOSs vs. distortion types between ACR-HR and SDSCE-DCS for pattern and non-pattern images.

Distortion Type	Blur	Additive Noise	JPEG	Contrast Change
Pattern	1	1	1	1
Non-pattern	1	1	0	0

TABLE 7. The sum of variances of MOSs between ACR-HR and SDSCE-DCS for different types of image distortions.

Distortion Type	Pattern		Non-pattern	
	ACR-HR	SDSCE-DCS	ACR-HR	SDSCE-DCS
Blur	41.09	**39.54**	**47.34**	47.66
Additive Noise	44.18	**42.26**	39.34	**37.34**
JPEG	41.43	**40.59**	**38.33**	39.25
Contrast Change	42.11	**37.34**	**37.22**	37.69

Therefore, it will cause a significant difference for the subjective scores the observers give to this type of scenes when viewing with or without the existence of the reference image. This is not unexpected since viewers indeed need a reference image to differentiate the quality difference between the distorted image and reference one when they view an image with so many similar patterns and simple colors. Hence, the variance of MOS will be larger when viewing this type of images without a reference to compare (i.e., ACR-HR). Table 5 shows the sum of variance is smaller for pattern image with contents #1, #3, #4, #6, #7, #8, #9, #12, #13, and #14 when evaluating by SDSCE-DCS, which also confirms the above results. The only exception is pattern image #10, which can be evaluated by ACR-HR because of smaller SoV.

C. IMAGE DISTORTION TYPES

From Table 6, the hypothesis test (h = 1) suggests that there exists a significant difference between two MOS groups obtained by ACR-HR and SDSCE-DCS for all distortion types on pattern images, and for *Blur* and *Additive noise* distortions on non-pattern images. Based on the observation from Table 6, we can conclude that the difference of two MOS sets is not significant for *JPEG distortion* and *Contrast Change* on non-pattern images. In addition, from Table 7, we note that for pattern images, the SoV is always smaller for all distortion types when subjective evaluation is conducted by SDSCE-DCS. However, the SoV is smaller for Blur distorted non-pattern images by using ACR-HR and for non-pattern images with Additive noise by using SDSCE-DCS. Hence, we can conclude SDECE-DCS is a better candidate for pattern images with all 4 types of distortions, while ACR-HR is more appropriate for evaluating non-pattern images with Blur, JPEG, and Contrast Change.

D. CORRELATION WITH IMAGE QUALITY METRICS (IQMS)

Based on the observations from above, we think SDSCE-DCS is a more suitable approach for evaluating pattern images instead of ACR-HR. The difference is little by using either ACR-HR or SDSCE-DCS on non-pattern images. However, the difference between both evaluation methods is large on

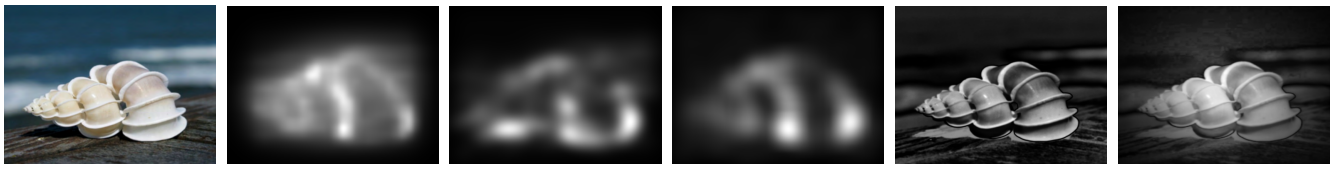

FIGURE 7. VS maps generated by using 5 different VS detection methods on pattern image. (a) Pattern image. (b)-(f) 5 different VS maps of (a). (a) Pattern. (b) GBVS. (c) ITTI. (d) HSSR. (e) FSRD. (f) SDSP.

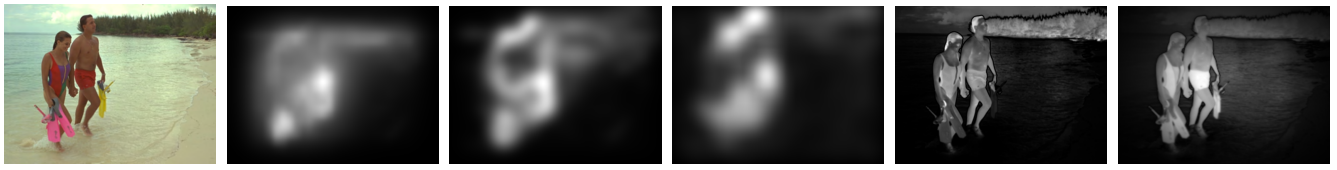

FIGURE 8. VS maps generated by using 5 different VS detection methods on non-pattern image. (a) Non-pattern image. (b)-(f) 5 different VS maps of (a). (a) Non-pattern. (b) GBVS. (c) ITTI. (d) HSSR. (e) FSRD. (f) SDSP.

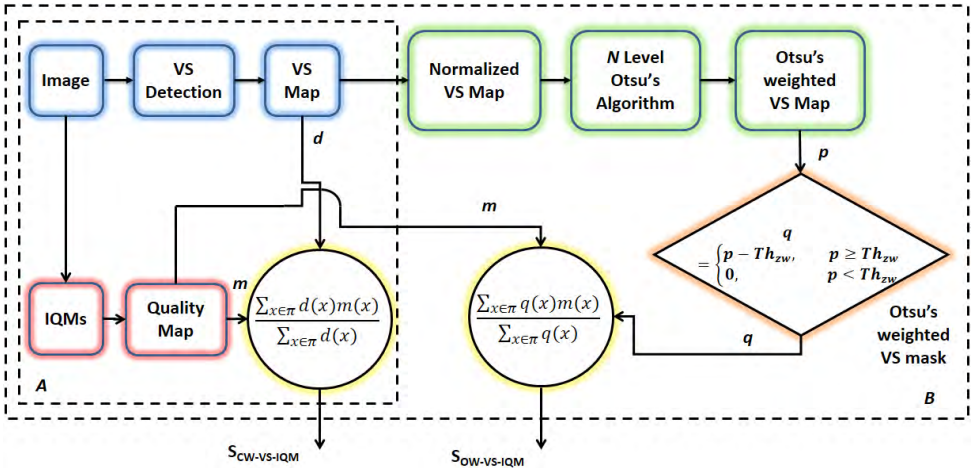

FIGURE 9. The block diagrams of CW-VS-IQM (block A) and OW-VS-IQM (block B).

TABLE 8. Correlations of scores computed by IQMs and MOSs obtained by SDSCE-DCS for pattern and non-pattern images.

IQM	Pattern			Non-pattern		
	PCC	SROCC	RMSE	PCC	SROCC	RMSE
PSNR	0.5750	0.5531	0.7477	0.3744	0.3935	0.8744
SSIM	0.7338	0.7239	0.6208	0.7591	0.7225	0.6139
FSIM	0.8128	0.8094	0.5324	0.7745	0.7753	0.5965

pattern images. In order to have a fair and the same standard comparison for both pattern and non-pattern images, we adopt the MOS results from the SDSCE-DCS method.

We also perform the tests for pattern and non-pattern images by using three full-reference image quality metrics (IQMs), including PSNR, SSIM [27], and FSIM [28]. The experimental results are summarized in Table 8. As we can observe in Table 8, FSIM ranks the first on the correlation coefficients [29], [30] (Pearson Correlation Coefficient (PCC), Spearman Rank Order Correlation Coefficient (SROCC)) and has the smallest Root-Mean-Squared Error (RMSE) [31] compared with other methods, which means it has the best performance to estimate the quality scores for both pattern and non-pattern images, while PSNR performs the worst.

Furthermore, we notice that PSNR and FSIM are more appropriate IQMs for predicting the quality scores of pattern images instead of non-pattern images because of their better correlation performance with MOS. However, SSIM does a better job at quality score prediction for non-pattern images.

IV. VISUAL SALIENCY EFFECTS

A. VISUAL SALIENCY CONSIDERATION

In this section, we want to investigate whether visual saliency [32], [33] plays an important role for predicting visual quality of pattern images. As we know, the visual saliency information has been incorporated into IQMs to improve the prediction performance of visual quality for

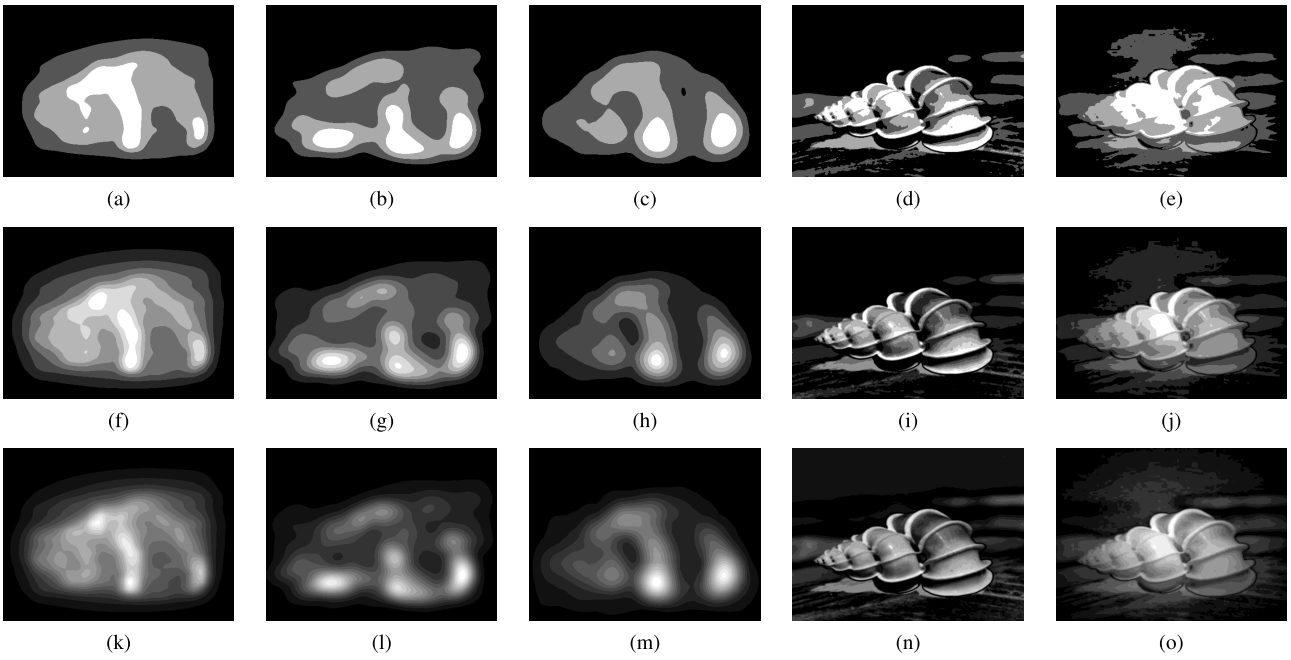

FIGURE 10. Otsu's weighted VS maps obtained by applying N level Otsu's algorithm on Fig. 7 (b)-(f). (a) GBVS, $N = 2^2 - 1$. (b) ITTI, $N = 2^2 - 1$. (c) HSSR, $N = 2^2 - 1$. (d) FSRD, $N = 2^2 - 1$. (e) SDSP, $N = 2^2 - 1$. (f) GBVS, $N = 2^3 - 1$. (g) ITTI, $N = 2^3 - 1$. (h) HSSR, $N = 2^3 - 1$. (i) FSRD, $N = 2^3 - 1$. (j) SDSP, $N = 2^3 - 1$. (k) GBVS, $N = 2^4 - 1$ (l) ITTI, $N = 2^4 - 1$ (m) HSSR, $N = 2^4 - 1$ (n) FSRD, $N = 2^4 - 1$ (o) SDSP, $N = 2^4 - 1$.

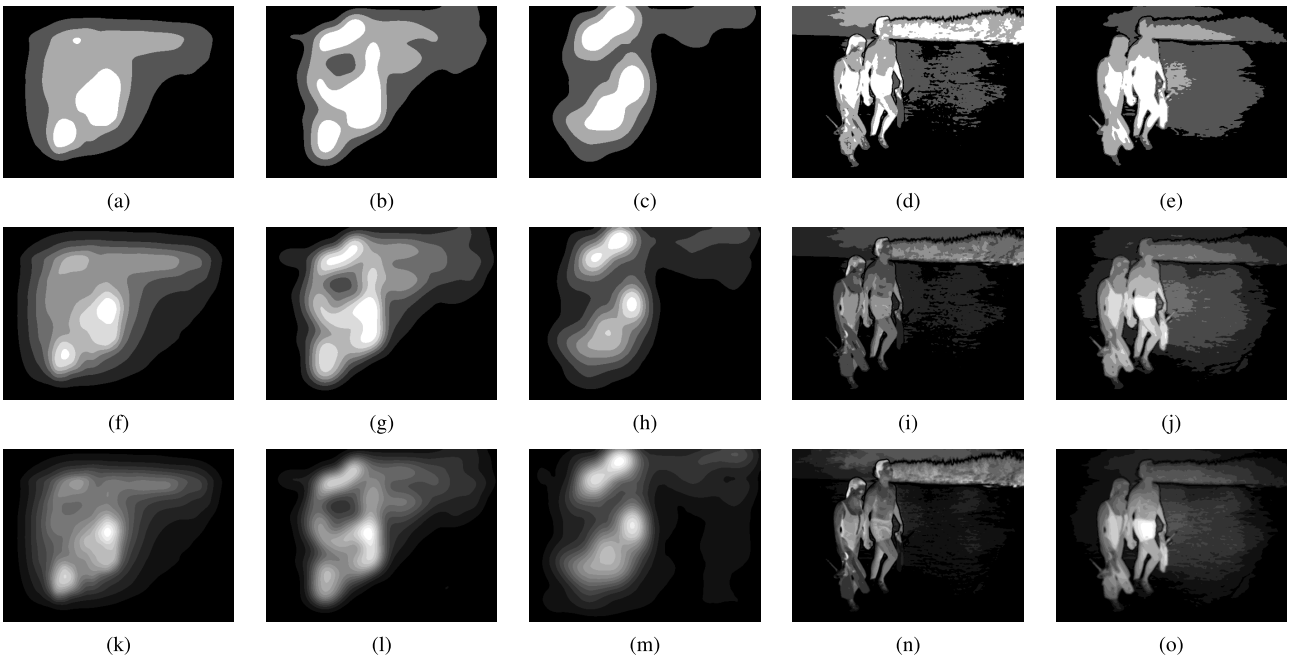

FIGURE 11. Otsu's weighted VS maps obtained by applying N level Otsu's algorithm on Fig. 8 (b)-(f). (a) GBVS, $N = 2^2 - 1$. (b) ITTI, $N = 2^2 - 1$. (c) HSSR, $N = 2^2 - 1$. (d) FSRD, $N = 2^2 - 1$. (e) SDSP, $N = 2^2 - 1$. (f) GBVS, $N = 2^3 - 1$. (g) ITTI, $N = 2^3 - 1$. (h) HSSR, $N = 2^3 - 1$. (i) FSRD, $N = 2^3 - 1$. (j) SDSP, $N = 2^3 - 1$. (k) GBVS, $N = 2^4 - 1$ (l) ITTI, $N = 2^4 - 1$ (m) HSSR, $N = 2^4 - 1$ (n) FSRD, $N = 2^4 - 1$ (o) SDSP, $N = 2^4 - 1$.

general (non-pattern) images [9]. In most of the cases, the visual saliency (VS) map is used as a weighting function at the stage of score pooling [34]. It also can be used as a feature map to characterize the quality of local image region [35]. Here, we adopt five best known and well-performed VS detection methods in this proposed system, including the VS model proposed by Itti *et al.* [36] for still images (ITTI), Graph-Based Visual Saliency (GBVS) [37], Highlighting Sparse Salient Regions (HSSR) proposed by Hou *et al.* [38], Frequency-tuned Salient Region

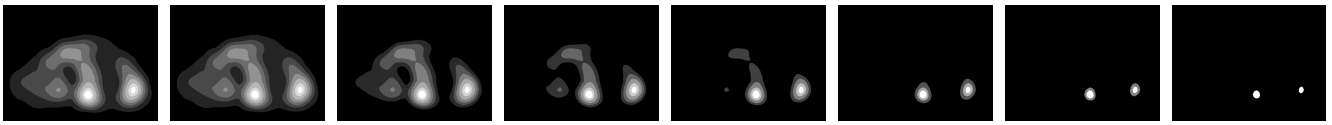

FIGURE 12. Otsu's weighted VS masks obtained by changing the Th_{zw} values for Fig. 10 (h). (a) $Th_{zw} = 0$. (b) $Th_{zw} = 1$. (c) $Th_{zw} = 2$. (d) $Th_{zw} = 3$. (e) $Th_{zw} = 4$. (f) $Th_{zw} = 5$. (g) $Th_{zw} = 6$. (h) $Th_{zw} = 7$.

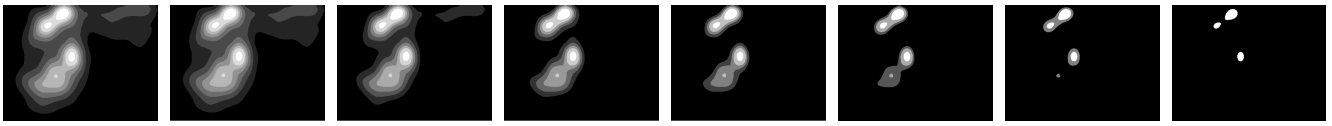

FIGURE 13. Otsu's weighted VS masks obtained by changing the Th_{zw} values for Fig. 11 (h). (a) $Th_{zw} = 0$. (b) $Th_{zw} = 1$. (c) $Th_{zw} = 2$. (d) $Th_{zw} = 3$. (e) $Th_{zw} = 4$. (f) $Th_{zw} = 5$. (g) $Th_{zw} = 6$. (h) $Th_{zw} = 7$.

Detection (FSRD) [39], and Saliency Detection by combining Simple Priors (SDSP) [40].

We apply the afore-mentioned VS detection methods to the pattern image in Fig. 7 (a) and non-pattern image in Fig. 8 (a). The resultant VS maps generated by five different VS detection algorithms are shown in Fig. 7 (b)-(f) and Fig. 8 (b)-(f). It can be observed different VS detection approaches cover different VS areas. In addition, the more salient the pixel is, the brighter the pixel in the VS map. Hence, the VS map mostly covers a smaller part of the original image. For instance, as shown in Fig. 8 (d), the VS map only considers the couple instead of both the ocean and the couple. This will affect the accuracy of image quality estimation.

B. VS-GUIDED IQMS

The VS detection method is performed on the test images to obtain the respective VS maps. Then, the obtained VS map X is converted to a normalized VS map Y by

$$y = \frac{x - min(X)}{max(X) - min(X)} \times 255, \tag{7}$$

where x and y represent any single pixel value in X and Y, respectively. Next, we apply the N level Otsu's algorithm [41] on normalized VS map to obtain a new VS map with $N + 1$ gray levels, called Otsu's weighted VS map. We denote the pixel value in Otsu's weighted VS map and Otsu's weighted VS mask as p and q, respectively. The q value is decided by comparing the p value with the Th_{zw} value via the following equation:

$$q = \begin{cases} p - Th_{zw} & p \geq Th_{zw} \\ 0 & p < Th_{zw}, \end{cases} \tag{8}$$

where $Th_{zw} = 0, 1, 2, \ldots, N$ is a threshold to assign zero values to the Otsu's weighted VS map. Finally, the Otsu's weighted VS mask q times the quality map m obtained by the IQM to form the Otsu's Weighted VS-guided IQM (OW-VS-IQM), whose quality score can be computed as below:

$$S_{OW-VS-IQM} = \frac{\sum_{x \in \pi} q(x)m(x)}{\sum_{x \in \pi} q(x)}, \tag{9}$$

where x represents the block or pixel in the entire image domain π. The detailed procedure is illustrated in the block B of Fig. 9. Here, we also present a Conventional Weighted VS-guided IQM (CW-VS-IQM) in block A of Fig. 9 for easy comparison. The resultant quality score can be calculated by

$$S_{CW-VS-IQM} = \frac{\sum_{x \in \pi} d(x)m(x)}{\sum_{x \in \pi} d(x)}, \tag{10}$$

where $d(x)$ is the conventional weight obtained from the VS map.

The $N(N = 2^2 - 1, 2^3 - 1, 2^4 - 1)$ level Otsu's algorithm is applied to Fig. 7 (b)-(f) and Fig. 8 (b)-(f) to divide the VS map into $N + 1$ discrete gray levels to form the Otsu's weighted VS maps, which are shown in Fig. 10 and Fig. 11. As we can observe in both figures, larger N values result in finer VS maps. In addition, we increase the Th_{zw} value from 0 to N to make the VS mask only keep the most salient objects or regions in the image. Thus, $N + 1$ different VS masks are created in Fig. 12 and Fig. 13 for Otsu's weighted VS maps in Fig. 10 (h) and Fig. 11 (h), respectively.

We use three well-known IQMs (PSNR, SSIM, and FSIM) to compute the quality map for each test image. Then the quality map times the VS map and Otsu's weighted VS mask respectively to realize the Conventional Weighted VS-guided IQM (CW-VS-IQM) and Otsu's Weighted VS-guided IQM (OW-VS-IQM). To have a clear comparison, we plot the SROCC performances of these three OW-VS-IQMs versus threshold of zero weight (Th_{zw}) on three different levels ($2^2, 2^3$, and 2^4) of VS maps for pattern images in Fig. 14(a)-(i), and non-pattern images in Fig. 14(j)-(r). As we can see in Fig. 14, each VS detection approach cannot work consistently well for all IQMs.

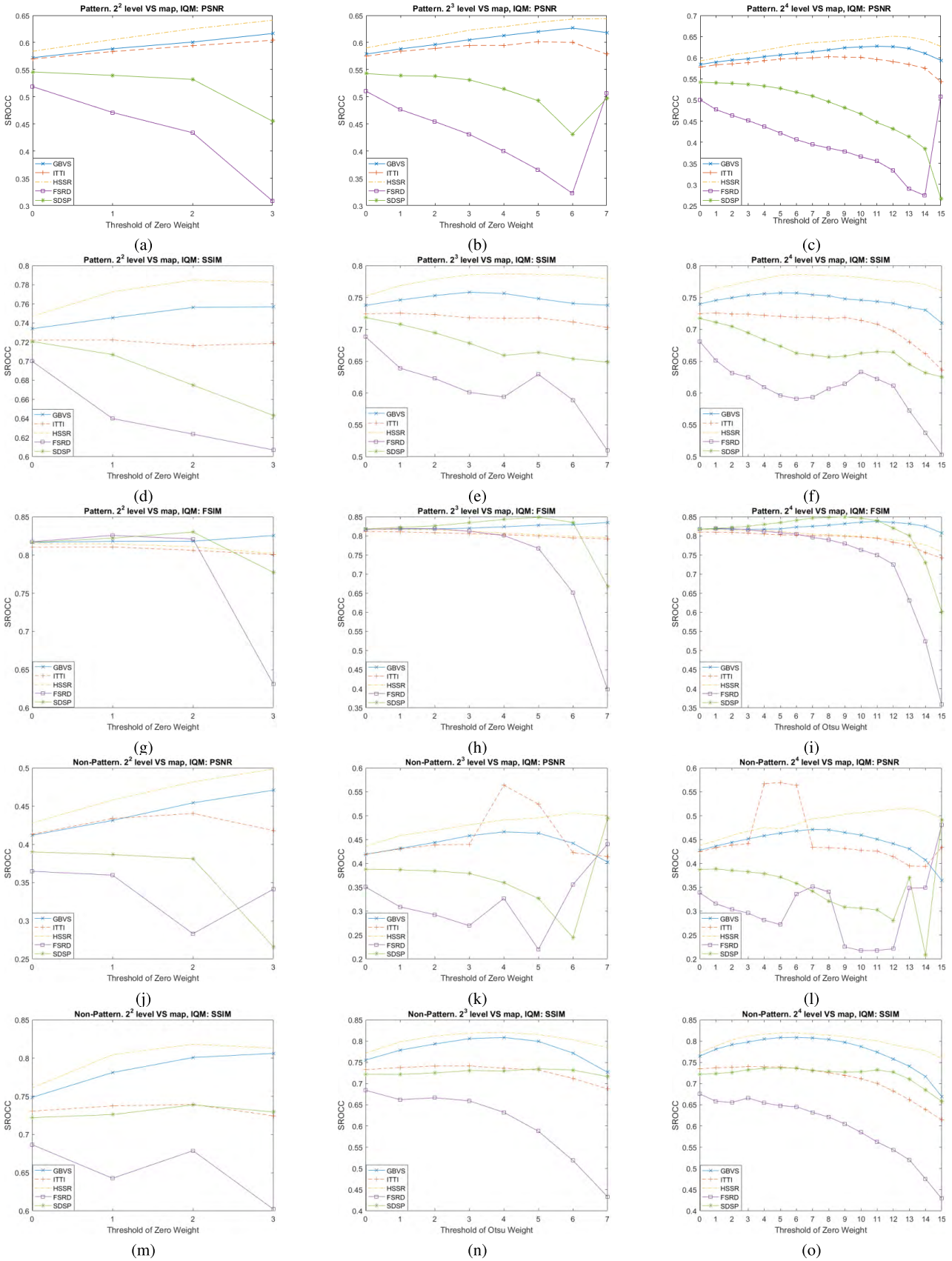

FIGURE 14. SROCC performance of OW-VS-IQM for PNP database. (a)-(i) Pattern images. (j)-(r) Non-pattern images.

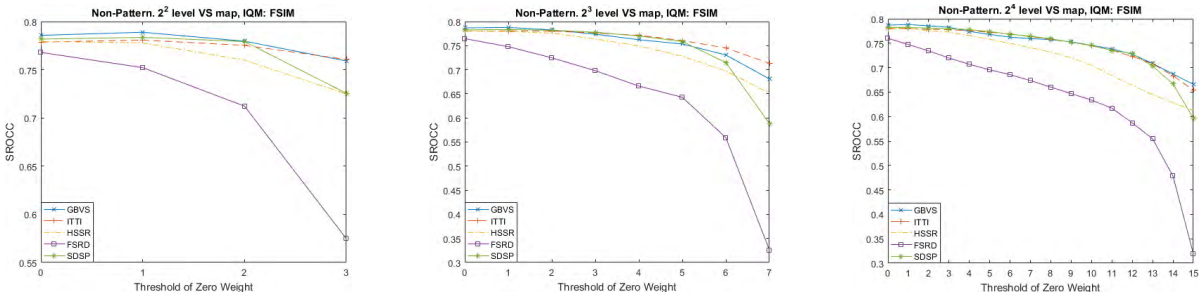

(p) (q) (r)

FIGURE 14. *(Continued.)* **SROCC performance of OW-VS-IQM for PNP database. (a)-(i) Pattern images. (j)-(r) Non-pattern images.**

TABLE 9. **The SROCC gain for all IQMs using the best matched VS detection method on pattern images.**

IQM	Original (A)	the best matched VS detection method	Conventional weighting (B)	Otsu's weighting (C)	N and Th_{zw} of Otsu's weighted VS map and mask	SROCC gain (B)-(A)	SROCC gain (C)-(A)	SROCC gain (C)-(B)
PSNR	0.5531	HSSR	0.5937	0.6505	$N = 2^4 - 1, Th_{zw} = 12$	0.0406	0.0974	0.0568
SSIM	0.7239	HSSR	0.7576	0.7869	$N = 2^3 - 1, Th_{zw} = 4$	0.0337	0.0630	0.0293
FSIM	0.8094	SDSP	0.8193	0.8498	$N = 2^4 - 1, Th_{zw} = 9$	0.0099	0.0404	0.0305

TABLE 10. **The SROCC gain for all IQMs using the best matched VS detection method on non-pattern images.**

IQM	Original (A)	the best matched VS detection method	Conventional weighting (B)	Otsu's weighting (C)	N and Th_{zw} of Otsu's weighted VS map and mask	SROCC gain (B)-(A)	SROCC gain (C)-(A)	SROCC gain (C)-(B)
PSNR	0.3935	ITTI	0.4287	0.5692	$N = 2^4 - 1, Th_{zw} = 5$	0.0352	0.1757	0.1405
SSIM	0.7225	HSSR	0.7781	0.8207	$N = 2^3 - 1, Th_{zw} = 4$	0.0556	0.0982	0.0426
FSIM	0.7753	GBVS	0.7876	0.7889	$N = 2^2 - 1, Th_{zw} = 1$	0.0123	0.0136	0.0013

TABLE 11. **Performance of CW-VS-IQMs and OW-VS-IQMs for pattern and non-pattern images.**

IQM	Pattern			Non-pattern		
	PCC	SROCC	RMSE	PCC	SROCC	RMSE
CW-VS-PSNR	0.6054	0.5937	0.7273	0.4090	0.4287	0.8605
CW-VS-SSIM	0.7714	0.7576	0.5815	0.8191	0.7781	0.5409
CW-VS-FSIM	0.8234	0.8193	0.5186	0.7828	0.7876	0.5867
OW-VS-PSNR	0.6550	0.6505	0.6906	0.4956	0.5692	0.8190
OW-VS-SSIM	0.8033	0.7869	0.5443	0.8512	0.8207	0.4949
OW-VS-FSIM	0.8489	0.8498	0.4831	0.7843	0.7889	0.5850

C. COMPARISON BETWEEN PATTERN AND NON-PATTERN IMAGES

We summarize the best matched VS detection algorithm, N and Th_{zw} values with respect to each IQM in Table 9 and Table 10 for pattern and non-pattern images, respectively. The SROCC performance gain for each IQM with respect to the used weighting method is also summarized in Tables 9 and 10.

For pattern images, HSSR is the best match of VS detection method for PSNR and SSIM, while SDSP is the most suitable one for FSIM. The SROCC gains are 0.0568, 0.0293 for PSNR and SSIM, which are not as significant as the improvement on non-pattern images. However, the Otsu's weighting boosts the SROCC performance by 0.0305 over conventional weighting for FSIM on pattern images. This improvement appears more significant than the one for FSIM on non-pattern images. For non-pattern images, ITTI, HSSR, and GBVS are the best matched VS detection methods for PSNR, SSIM and FSIM. The SROCC value increases by 0.1405 when Otsu's weighting is used to replace the conventional weighting for PSNR. But the SROCC performance is almost the same (i.e., increase by 0.0013 in SROCC value) for FSIM using either conventional or Otsu's weighting.

As we can observe from Tables 9 and 10, the value of threshold of zero weight (Th_{zw}) is larger for pattern images than non-pattern images. This is probably because the pattern images have repeated objects or periodic shapes on them. Therefore, the IQMs can just focus on the most salient objects or regions rather than whole area to complete the evaluation of image quality by setting most of the weights to zeros (i.e., for non-salient areas) in the Otsu's weighted VS mask.

In the end, we list the PCC, SROCC, and RMSE performances for CW-VS-IQMs and OW-VS-IQMs in Table 11. The experimental results show the OW-VS-FSIM performs the best for pattern images, while the OW-VS-SSIM ranks number one for non-pattern images. Additionally, the CW-VS-PSNR has the worst performance among all compared IQMs for pattern and non-pattern images. Moreover, comparing Table 11 with Table 8, we find out the performance of visual quality prediction for IQMs improves by combining the VS map with the conventional weighting. And the results can be boosted further by using Otsu's weighted VS mask.

V. CONCLUSION

In this paper, we perform subjective evaluations on pattern and non-pattern images in PNP image quality database by both ACR-HR and SDSCE-DCS. The experimental results show that the differences between two sets of MOSs obtained from both evaluation methods are significant for image types, image contents, and several specific distortion types. For instance, the sum of variances is obviously smaller for conducting subjective viewing tests on pattern images with SDSCE-DCS rather than ACR-HR. Also, the ACR-HR is more appropriate for evaluating non-pattern images with Blur, JPEG, and Contrast Change than SDSCE-DCS. However, the SDSCE-DCS is a better candidate for performing viewing test on pattern images with all four types of distortions. In other words, for most of the cases, non-pattern images can be viewed with a simpler approach (e.g., ACR-HR) to simplify the viewing process and save time.

Furthermore, we test several IQMs on pattern and non-pattern images, respectively. Five popular and well-performed VS detection models are introduced to the existing IQMs to boost the performance of predicting image quality. We discover that each IQM has its corresponding best matched VS detection approach and threshold value of zero weight. For example, HSSR is the perfect match for SSIM on both pattern and non-pattern images. In addition, We need a larger value to serve as the threshold of zero weight in the Otsu's weighted VS mask for pattern images. This means the salient regions affect human's perception of image quality more than non-salient regions on pattern images. This conclusion also justifies the VS information is more crucial for evaluating the images with repeated objects or periodic shapes (i.e., pattern images).

We also propose an Otsu's weighted VS mask method to boost the performance of IQMs. The experimental results show that it indeed improve the correlation performance between subjective scores and objective scores obtained from IQMs further than the conventional VS map method.

REFERENCES

[1] W. Lin and C.-C. Jay Kuo, "Perceptual visual quality metrics: A survey," *J. Visual Commun. Image Representation*, vol. 22, no. 4, pp. 297–312, 2011.

[2] T.-J. Liu, W. Lin, and C.-C. J. Kuo, "A multi-metric fusion approach to visual quality assessment," in *Proc. 3rd Int. Workshop Qual. Multimedia Exper. (QoMEX)*, Sep. 2011, pp. 72–77.

[3] M. Narwaria and W. Lin, "SVD-based quality metric for image and video using machine learning," *IEEE Trans. Syst., Man, Cybern. B, Cybern.*, vol. 42, no. 2, pp. 347–364, Apr. 2012.

[4] T.-J. Liu, W. Lin, and C.-C. J. Kuo, "Image quality assessment using multi-method fusion," *IEEE Trans. Image Process.*, vol. 22, no. 5, pp. 1793–1807, May 2013.

[5] T. Liu, K. Liu, J. Lin, W. Lin, and C.-C. J. Kuo, "A paraboost method to image quality assessment," *IEEE Trans. Neural Netw. Learn. Syst.*, vol. 28, no. 1, pp. 107–121, Jan. 2017.

[6] T.-J. Liu and K.-H. Liu, "No-reference image quality assessment by wide-perceptual-domain scorer ensemble method," *IEEE Trans. Image Process.*, vol. 27, no. 3, pp. 1138–1151, Mar. 2018.

[7] S. Chikkerur, V. Sundaram, M. Reisslein, and L. J. Karam, "Objective video quality assessment methods: A classification, review, and performance comparison," *IEEE Trans. Broadcast.*, vol. 57, no. 2, pp. 165–182, Jun. 2011.

[8] M. Liu, G. Zhai, S. Tan, Z. Zhang, K. Gu, and X. Yang, "HDR2014—A high dynamic range image quality database," in *Proc. IEEE Int. Conf. Multimedia Expo Workshops (ICMEW)*, Jul. 2014, pp. 1–6.

[9] K. Gu *et al.*, "Saliency-guided quality assessment of screen content images," *IEEE Trans. Multimedia*, vol. 18, no. 6, pp. 1098–1110, Jun. 2016.

[10] T.-J. Liu, K.-H. Liu, H.-H. Liu, and S.-C. Pei, "Comparison of subjective viewing test methods for image quality assessment," in *Proc. IEEE Int. Conf. Image Process. (ICIP)*, Sep. 2015, pp. 3155–3159.

[11] J. Y. Lin, R. Song, T. Liu, H. Wang, and C.-C. J. Kuo, "MCL-V: A streaming video quality assessment database," *J. Vis. Commun. Image Represent.*, vol. 30, pp. 1–9, Jul. 2015.

[12] T.-J. Liu, W. Lin, and C.-C. J. Kuo, "Recent developments and future trends in visual quality assessment," in *Proc. Asia-Pacific Signal Inf. Process. Assoc. Annu. Submit Conf. (APSIPA ASC)*, Xi'an, China, Oct. 2011, pp. 1–10.

[13] T.-J. Liu, Y.-C. Lin, W. Lin, and C.-C. J. Kuo, "Visual quality assessment: Recent developments, coding applications and future trends," *APSIPA Trans. Signal Inf. Process.*, vol. 2, p. e4, Jul. 2013. [Online]. Available: http://journals.cambridge.org/article_S204877031300005X

[14] International Telecommunication Union, Recommendation ITU-R BT.500-13, Jan. 2012, "Methodology for the subjective assessment of the quality of television pictures."

[15] International Telecommunication Union, Recommendation ITU-T P.910, Apr. 2008, "Subjective video quality assessment methods for multimedia applications."

[16] M. H. Pinson and S. Wolf, "Comparing subjective video quality testing methodologies," *Proc. SPIE*, vol. 5150, pp. 573–582, Jun. 2003.

[17] *50 Dazzling Images of Patterns*. [Online]. Available: http://photography.tutsplus.com/articles/50-dazzling-images-of-patterns–photo-8567

[18] *Tampere Image Database 2013*. [Online]. Available: http://www.ponomarenko.info/tid2013.htm

[19] *Kodak Database*. [Online]. Available: http://r0k.us/graphics/kodak/

[20] *PNP Image Quality Database*. [Online]. Available: https://sites.google.com/site/tjliu412/home/downloads/pnp_iq_database

[21] D. M. Rouse, R. Pépion, P. Le Callet, and S. S. Hemami, "Tradeoffs in subjective testing methods for image and video quality assessment," *Proc. SPIE*, vol. 7527, p. 75270F, Jan. 2010.

[22] Q. Huynh-Thu, M.-N. Garcia, F. Speranza, P. Corriveau, and A. Raake, "Study of rating scales for subjective quality assessment of high-definition video," *IEEE Trans. Broadcast.*, vol. 57, no. 1, pp. 1–14, Mar. 2011.

[23] L. Ma, W. Lin, C. Deng, and K. N. Ngan, "Image retargeting quality assessment: A study of subjective scores and objective metrics," *IEEE J. Sel. Topics Signal Process.*, vol. 6, no. 6, pp. 626–639, Oct. 2012.

[24] International Telecommunication Union, Recommendation ITU-R BT.2022, Aug. 2012, "General viewing conditions for subjective assessment of quality of SDTV and HDTV television pictures on flat panel displays."

[25] K.-H. Liu, T.-J. Liu, H.-H. Liu, and S.-C. Pei, "Facial makeup detection via selected gradient orientation of entropy information," in *Proc. IEEE Int. Conf. Image Process. (ICIP)*, Sep. 2015, pp. 4067–4071.

[26] S. A. Glantz, *Primer of Biostatistics*, 6th ed. New York, NY, USA: McGraw-Hill, 2005.

[27] Z. Wang, A. C. Bovik, H. R. Sheikh, and E. P. Simoncelli, "Image quality assessment: From error visibility to structural similarity," *IEEE Trans. Image Process.*, vol. 13, no. 4, pp. 600–612, Apr. 2004.

[28] L. Zhang, L. Zhang, X. Mou, and D. Zhang, "FSIM: A feature similarity index for image quality assessment," *IEEE Trans. Image Process.*, vol. 20, no. 8, pp. 2378–2386, Aug. 2011.
[29] Video Quality Experts Group, "Final report from the video quality experts group on the validation of objective models of video quality assessment, phase I," Video Quality Experts Group, Ottawa, ON, Canada, Tech. Rep., Mar. 2000. [Online]. Available: http://www.its.bldrdoc.gov/vqeg/projects/frtv_phaseI
[30] T.-J. Liu, K.-H. Liu, and H.-H. Liu, "Correlation coefficients: Reliable performance indices for visual quality assessment?" *Int. J. Sci. Prog. Res.*, vol. 30, no. 1, pp. 1–5, 2016.
[31] Video Quality Experts Group, "Final report from the video quality experts group on the validation of objective models of video quality assessment, phase II," Video Quality Experts Group, Hillsboro, OR, USA, Tech. Rep., Aug. 2003. [Online]. Available: http://www.its.bldrdoc.gov/vqeg/projects/frtv_phaseII
[32] Y. Fang, W. Lin, B.-S. Lee, C.-T. Lau, Z. Chen, and C.-W. Lin, "Bottom-up saliency detection model based on human visual sensitivity and amplitude spectrum," *IEEE Trans. Multimedia*, vol. 14, no. 1, pp. 187–198, Feb. 2012.
[33] N. Imamoglu, W. Lin, and Y. Fang, "A saliency detection model using low-level features based on wavelet transform," *IEEE Trans. Multimedia*, vol. 15, no. 1, pp. 96–105, Jan. 2013.
[34] J. Y. Lin, T.-J. Liu, W. Lin, and C.-C. J. Kuo, "Visual-saliency-enhanced image quality assessment indices," in *Proc. Asia–Pacific Signal Inf. Process. Assoc. Annu. Summit Conf. (APSIPA)*, Oct./Nov. 2013, pp. 1–4.
[35] L. Zhang, Y. Shen, and H. Li, "VSI: A visual saliency-induced index for perceptual image quality assessment," *IEEE Trans. Image Process.*, vol. 23, no. 10, pp. 4270–4281, Aug. 2014.
[36] L. Itti, C. Koch, and E. Niebur, "A model of saliency-based visual attention for rapid scene analysis," *IEEE Trans. Pattern Anal. Mach. Intell.*, vol. 20, no. 11, pp. 1254–1259, Nov. 1998.
[37] J. Harel, C. Koch, and P. Perona, "Graph-based visual saliency," in *Proc. NIPS*, vol. 1, no. 2, 2006, pp. 545–552.
[38] X. Hou, J. Harel, and C. Koch, "Image signature: Highlighting sparse salient regions," *IEEE Trans. Pattern Anal. Mach. Intell.*, vol. 34, no. 1, pp. 194–201, Jan. 2012.
[39] R. Achanta, S. Hemami, F. Estrada, and S. Susstrunk, "Frequency-tuned salient region detection," in *Proc. IEEE Conf. Comput. Vis. Pattern Recognit. (CVPR)*, Jun. 2009, pp. 1597–1604.
[40] L. Zhang, Z. Gu, and H. Li, "SDSP: A novel saliency detection method by combining simple priors," in *Proc. 20th IEEE Int. Conf. Image Process. (ICIP)*, Sep. 2013, pp. 171–175.
[41] N. Otsu, "A threshold selection method from gray-level histograms," *IEEE Trans. Syst., Man, Cybern.*, vol. SMC-9, no. 1, pp. 62–66, Jan. 1979.

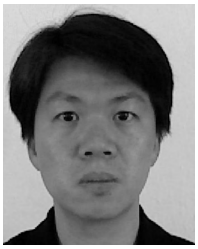

TSUNG-JUNG LIU (S'10–M'14) received the B.S. degree in electrical engineering from National Tsing Hua University, Hsinchu, Taiwan, in 1998, the M.S. degree in communication engineering from National Taiwan University, Taipei, Taiwan, in 2001, and the Ph.D. degree in electrical engineering from the University of Southern California, Los Angeles, CA, USA, in 2014.

He is currently an Assistant Professor with the Department of Electrical Engineering and Graduate Institute of Communication Engineering, National Chung Hsing University, Taichung, Taiwan. His research interests include computer vision, perceptual image/video processing, visual quality assessment, and big data analytics.